Thermal Conductivity of Polycrystalline Dysprosium from 5 to 305°K

R. V. COLVIN AND SIGURDS ARAJS
Edgar C. Bain Laboratory, United States Steel Corporation, Research Center for Fundamental Research, Monroeville, Pennsylvania

(Received 2 October 1963)

Thermal conductivity of polycrystalline dysprosium has been studied between 5 and 305°K. An abrupt decrease in the thermal conductivity occurs at the ferromagnetic-antiferromagnetic transformation. The transition from the antiferromagnetic to the paramagnetic state causes a gradual increase in the thermal conductivity with increasing temperatures. The Lorenz number of dysprosium has been calculated as a function of temperature. It is concluded that in addition to the electronic thermal conductivity there is considerable lattice conductivity and possibly some magnon conductivity. An apparatus for determining the thermal conductivity of solids from liquid-helium to room temperatures is briefly described.

INTRODUCTION

THERMAL conductivity measurements on the rare-earth metals from liquid-helium to room temperatures have not been done before. Lanthanum and cerium are the only rare-earth metals whose thermal conductivities have been determined[1] over a small temperature range at low temperatures. Thermal conductivities of some other rare-earth metals have been determined at room temperatures.[2] Our purpose in undertaking the experiments reported here was to enlarge the knowledge of heat transport of the rare-earth metals. Most of these elements undergo cooperative magnetic phenomena resulting in various types of antiferromagnetic and ferromagnetic ordering at low temperatures. This magnetic behavior stems from the localized $4f$ electrons in these elements. It is known that the electrical conduction in the rare-earth metals is greatly influenced by the magnetic state of the metal. Thus, we may expect a similar behavior with respect to the thermal conductivity.

In this paper we describe briefly the experimental techniques used to study the thermal conductivity of metals from liquid-helium to room temperatures. The measurements on polycrystalline dysprosium are discussed in detail.

EXPERIMENTAL CONSIDERATIONS

The thermal conductivity cell (stationary method) used in this investigation is shown in Fig. 1, and is similar to that used by Born *et al.*[3] for their thermoelectric power studies of the rare-earth metals.

Sample S, 0.476 cm in diameter and about 5 cm long, is mounted in the inner copper can C_1 which acts as a heat sink and also as a radiation shield. This can is attached to the outer can C_2 (also made of copper) by means of a short stainless steel tubing T_1 (o.d. $\frac{3}{8}$ in., wall 0.010 in.) which provides a high-resistance thermal path between the two cans. Normally, the chamber enclosed by this tubing is evacuated through another stainless steel tubing T_2 (o.d. $\frac{3}{16}$ in., wall 0.010 in.). Thus the inner can can be conveniently kept, using a manganin heater H_1, above the temperature of the liquid (helium, hydrogen, or nitrogen) surrounding the outer can C_2. If a better heat leak between the cans C_1 and C_2 is needed, then the chamber enclosed by T_1 can be filled with helium gas. The can C_1 has a copper door (not shown in Fig. 1) which allows the sample to be placed inside this container. The door is thermally anchored (by means of copper wires) to the rest of the can C_1. The thermal conductivity cell can be evacuated through the stainless steel tubing T_2 (o.d. $\frac{3}{4}$ in., wall 0.016 in.) which is soldered in the copper lid. The outer can is attached to this lid and the inner assembly by means of Wood's metal seal W.

The temperature gradient along the sample S is established using a heater H_2. It consists of a noninductively wound quadruple-Formvar manganin wire (No. 30, total resistance about 95 Ω at room temperature) on a light (small mass) aluminum cap. This heater is tightly clamped to the sample as shown in Fig. 1. The other end of the sample is fastened to the heat sink by means of a copper clamp K. The temperature difference along the sample is determined with a copper-constantan differential thermocouple. The thermal contacts of this couple to the sample are made as follows. A short section of the stainless steel tubing (o.d. $\frac{3}{16}$ in., wall 0.010 in., length $\frac{3}{16}$ in.) is filled with a Saureisen (No. 29) paste, then dried and baked. After this a small hole is drilled into the hardened Saureisen section. The differential thermocouple junctions (No. 38 copper and No. 30 constantan wires) are placed and glued into the holes using a GE adhesive (No. 7031). The sections of the stainless steel tubing, tinned before the above-described procedure, are soldered to copper wires (No. 26) spot welded to the sample. The absolute temperature of the sample is determined using the copper-constantan thermocouple Th_2 soldered at the thermal contact nearest to the heat sink. All the thermocouple wires and the current and potential leads from the heater H_2 are taken out from the inner can through two copper elbows E (only one is shown in Fig. 1) and are thermally grounded by wrapping around the elbows and

[1] H. M. Rosenberg, Phil. Trans. Roy. Soc. London 247, 441 (1955).
[2] S. Legvold and F. M. Spedding, United States Atomic Energy Commission Report ISC-508, 1954 (unpublished).
[3] H. J. Born, S. Legvold, and F. H. Spedding, J. Appl. Phys. 32, 2543 (1961).

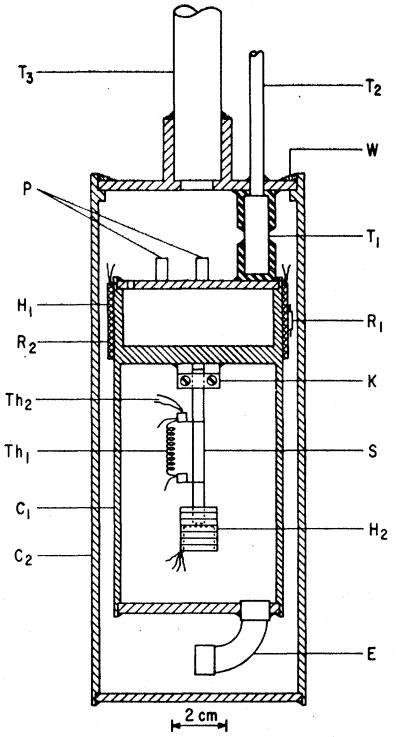

FIG. 1. Thermal conductivity cell. T_1, T_2, T_3—stainless steel tubing. W—Wood's metal. P—thermal grounding posts. H_1, H_2—heaters. R_1—carbon sensing element. R_2—copper sensing element. Th_1—differential thermocouple. Th_2—thermocouple. K—clamp. S—sample. C_1—inner can. C_2—outer can. E—copper elbow.

the grounding posts P and then glueing with a GE adhesive. In order to reduce the radiation losses, the walls of the cans C_1 and C_2 have been chrome-plated. The heater H_2 is wrapped with an aluminum foil. The possibility of some radiation leaving the inner chamber through the elbows E is eliminated by using aluminum foil shields.

The temperatures of the inner can C_1 are obtained using the heater H_1 wound from cotton covered No. 29 manganin wire. The room-temperature resistance of this heater is about 85 Ω. The temperature of the inner can is kept constant within ± 0.01°K by means of an electronic controller. Either a carbon resistor R_1 (Allen-Bradley, 0.1 W, 22 Ω at room temperature) or a copper resistor R_2 (wound from No. 38 Nyclad copper wire, 105 Ω at room temperature), depending upon the temperatures to be controlled, is used as a sensing unit. The copper or carbon resistor is in one arm of the Wheatstone bridge circuit, with the input of a Brown servo-amplifier (358816) connected at the null detector position. This amplifier controls a Helipot by means of a servomotor. An independently programmed power supply connected to this Helipot supplies power to the heater. One thus obtains temperature control of the can C_1. It is also possible to control temperature on an on-off schedule with another servomotor equipped with a mechanical arm that operates a switch. Since it is useful to change the temperatures of the inner can as quickly as possible, automatic switching apparatus has been incorporated so that the can C_1 may be heated to a slightly higher temperature, then cooled to the desired temperature, cycled on the on-off basis to stabilize the temperature, and then switched to the proportional control with the servomechanism positioned properly to begin the control. The reverse mode of this type of control is also possible for measurements to be made with decreasing temperatures.

The power to the heater H_2 on the sample is provided by a constant voltage power supply (Power Designs, model TW-4005). When the temperature of the sink is increased, the previously established steady-state temperature gradient along the sample tends to decrease. In order to correct partially for this change, the following technique is used. A meter relay, coupled with a Keithley 149 milli-microvoltmeter, causes a preselected increase in the electrical current through the heater when the temperature differential has dropped to a certain value. This value was determined by trial to re-establish steady state in a reasonably short time. After this, the power supply atuomatically delivers the selected current for the chosen temperature gradient. This procedure speeds up the achievement of the steady-state heat flow in the sample after the temperature of the inner can is changed.

The temperature difference between the thermal potential contacts was measured with a Rubicon microvolt potentiometer (2768), using a Rubicon photoelectric galvanometer (3550) combined with a Leeds and Northrup dc microvolt amplifier (9835-B) as a null detector. With this equipment it was possible to measure reliably ± 0.01 μV. The thermoelectric voltages of the thermocouple Th_2 were measured with a Tinsley Diesselhorst potentiometer (3589-S). The current and the voltage of the heater H_2 were determined using Rubicon type B potentiometers.

The thermal conductivity of the sample was calculated from the equation

$$\lambda = \dot{Q} l / (A \Delta T), \qquad (1)$$

where $\dot{Q}$ is the power dissipated in the heater, l the distance between the thermal contacts, A the cross-sectional area of the sample, and ΔT the temperature difference between the thermal contacts under the steady-state conditions. During this experiment the quantity ΔT ranged from 1—4°K. The conductive heat losses through the wires were estimated to be negligible. Since the vacuum in the cell during the experiment was about 6×10^{-6} mm Hg, the gaseous conduction losses also were negligible. The correction for the radiation losses above liquid nitrogen temperatures were made in the standard manner. The majority of the thermal conductivity observations have an estimated error of about 2% and appear to be reproducible to at least this accuracy.

The sample of dysprosium used in this study was

purchased from St. Eloi Corporation. Its residual electrical resistivity at 4.2°K was found to be 9.55 $\mu\Omega$ cm. The analysis of this material is presented in Table I.

TABLE I. Analysis of dysprosium.[a]

Ta(0.2), Tb(0.1), Ca(0.05), Ho(0.05), Er(0.02), Si(0.02), Y(0.02), Fe(0.01), Mg(0.01), Cu(trace), La(trace).
Not detected: Ce, Co, Cr, Mo, Ti, V, W, Yb, Zr.

[a] The number in the bracket gives the amount of the impurity in % by weight.

The high-temperature paramagnetic properties of the same sample have been studied before.[4]

RESULTS AND DISCUSSION

Figure 2 shows the thermal conductivity (λ) and the electrical resistivity (ρ) of this sample of dysprosium as a function of temperature. The resistivity data, using the same sample, were obtained about three years before the heat transport studies. The electrical resistivity measurements were made in an apparatus described elsewhere.[5]

It can be seen from Fig. 2 that the thermal conductivity rises rapidly with increasing temperatures, reaches a maximum at about 25°K, and then decreases. The influence of the ferromagnetic-antiferromagnetic and the antiferromagnetic-paramagnetic transitions on the thermal and electrical conductivities are clearly observable. Below about 85°K, dysprosium is ferromagnetic,[6–8] with the magnetic moments parallel or closely parallel to the hexagonal layers. Between 85 and 180°K, the antiferromagnetic structure[6–8] is a helical moment configuration, with the c axis as the screw axis. That is, the moments are oriented in a direction perpendicular to the hexagonal c axis, and form ferromagnetic sheets of moments in the hexagonal layers with a specific angle of rotation (the turn angle) between moments in adjacent layers. The turn angle is a function of temperature. Above 180°K, dysprosium is paramagnetic, i.e., the magnetic moments arising from the localized $4f$ electrons are uncorrelated. These magnetic transformations cause a small step in the thermal conductivity at about 85°K and a considerable increase (in comparison with the thermal conductivity in the antiferromagnetic state) with increasing temperatures above 180°K. The influence of the magnetic states on the electrical resistivity is also demonstrated in Fig. 2.

Although a large amount of work has been done on the thermal transport behavior in solids, the influence of various magnetic states on the thermal conductivity is a

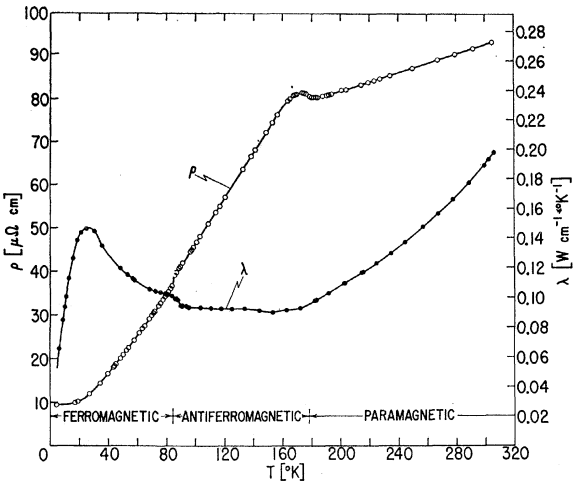

FIG. 2. Thermal conductivity and electrical resistivity of polycrystalline dysprosium as a function of temperature.

quite unexplored phenomenon from both experimental and theoretical points of view. In fact, we are not aware of any previous study of the thermal conductivity in a metal over the temperature range where it exhibits an antiferromagnetic transition. A theory of the thermal conductivity applicable to the rare earth metals possessing certain magnetic structures has not been developed yet. These structures not only can cause energy gaps in the spin-wave spectra[9] but also can modify the Fermi surface.[10–12] Thus a quantitative detailed analysis of our data is not possible at the present time. However, we can make some qualitative statements about the unusual thermal conductivity curve for dysprosium as shown in Fig. 2.

In the paramagnetic region, the total electrical resistivity of polycrystalline dysprosium can be approximately written as

$$\rho^P=\rho_0+\rho_m{}^P+\rho_l{}^P, \tag{2}$$

where ρ_0 is the residual electrical resistivity due to the chemical and structural impurities, $\rho_m{}^P$ the magnetic resistivity, and $\rho_l{}^P$ the intrinsic electrical resistivity. The quantity $\rho_m{}^P$, resulting from the scattering of the conduction electrons by the disordered magnetic moments in the paramagnetic region, can be considered to be independent of temperature. The intrinsic resistivity $\rho_l{}^P$ is due to the electron-phonon scattering and thus is a function of temperature. Ideally, this resistivity is describable by the Bloch-Grüneisen theory which reduces to $\rho_l \propto T^5$ for $T \ll \theta$, and $\rho_l \propto T$ for $T \gg \theta$, θ being the Debye temperature. It is believed that the Bloch-Grüneisen formulation is not a good theory for

[4] S. Arajs and R. V. Colvin, J. Appl. Phys. **32**, 336S (1961).
[5] S. Arajs, J. Appl. Phys. **32**, 97 (1961).
[6] D. R. Behrendt, S. Legvold, and F. M. Spedding, Phys. Rev. **109**, 1544 (1958).
[7] W. C. Koehler, E. O. Wollan, M. K. Wilkinson, and J. W. Cable, in *Rare Earth Research*, edited by E. V. Kleber (The MacMillan Company, New York, 1961).
[8] M. K. Wilkinson, W. C. Koehler, E. O. Wollan, and J. W. Cable, J. Appl. Phys. **32**, 48S (1961).
[9] A. R. Mackintosh, Phys. Letters **3**, 140 (1963).
[10] A. R. Mackintosh, in *Rare Earth Research*, edited by J. F. Nachman and C. E. Lundin (Gordon and Breach Science Publishers, New York, 1962), p. 272.
[11] A. W. Overhauser, J. Appl. Phys. **34**, 1019 (1963).
[12] A. Arrott, in *Magnetism: A Treatise on Modern Theory and Materials* (Academic Press Inc., New York, to be published).

the electron-phonon resistivity in the rare-earth metals[13] because of the interband scattering and a possible rapidly varying electronic density of states curve with energy. Incidently, we have not included in Eq. (2) a term representing the resistivity contribution resulting from either the elastic or inelastic scattering of the conduction electrons by the localized $4f$ electrons.[14,15] This is justified on the basis that we neglect the electric crystalline fields in dysprosium, and the energy level picture of the free tripositive dysprosium ions is such that no contributions to the resistivity would result at room temperatures.

Similarly, the electronic thermal resistivity of dysprosium in the paramagnetic state can be approximated by the equation

$$\eta^{P,e}=\eta_0{}^e+\eta_m{}^{P,e}+\eta_l{}^{P,e}, \tag{3}$$

where $\eta_0{}^e$ is the impurity thermal resistivity, $\eta_m{}^{P,e}$ the magnetic part similar to $\rho_m{}^P$, and $\eta_l{}^{P,e}$ the electronic thermal resistivity due to the scattering by phonons. The quantity $\eta_0{}^e$ is related to ρ_0 by means of the Wiedemann–Franz law, i.e.,

$$\eta_0{}^e=\rho_0/LT, \tag{4}$$

where T is the absolute temperature and L is the Lorentz number. Since the same assumption (the relaxation time is the same for both the electric and thermal transport by electrons) would be expected to hold for the scattering of electrons by the disordered magnetic moments, we can write

$$\eta_m{}^{P,e}=\rho_m{}^P/LT. \tag{5}$$

Moreover, let us assume that in the paramagnetic region the elastic scattering predominates so that

$$\eta_l{}^{P,e}=\rho_l{}^P/LT. \tag{6}$$

Then the thermal conductivity of electrons is

$$\lambda^{P,e}=LT/\rho^P. \tag{7}$$

The total thermal conductivity (λ^P) of dysprosium in the paramagnetic state should, in principle, include a term due to the lattice conduction ($\lambda^{P,l}$), i.e.,

$$\lambda^P=\lambda^{P,e}+\lambda^{P,l}. \tag{8}$$

By using the experimental data shown in Fig. 2, we find that $\lambda^{P,l}\approx 0.11$ W cm^{-1} °K^{-1} at 300°K and $\lambda^{P,l}\approx 0.05$ W cm^{-1} °K^{-1} at 200°K. Such values are not unreasonable, especially if one emphasizes the crudeness of the calculations. The lattice thermal conductivities for other metals are of the same order of magnitude.[16]

In order to get some insight about the thermal conductivity of dysprosium, especially at lower temperatures, we have calculated the Lorenz number (Fig. 3) defined as

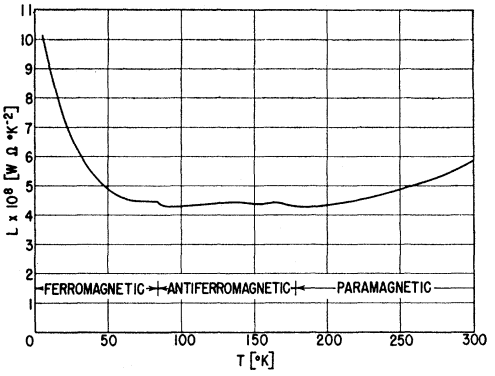

FIG. 3. Lorenz number of dysprosium as a function of temperature.

$$L=\lambda\rho/T, \tag{9}$$

where λ and ρ are the measured thermal conductivity and the electrical resistivity at the temperature T, respectively. For usual metals, i.e., those with negligible lattice thermal conductivity, the Lorentz number at low temperatures is very close to the theoretical value[17] 2.45×10^{-18} W Ω °K^{-2}. As the temperature increases, the quantity L decreases, reaches a minimum depending upon the purity of the sample, and then increases back to the theoretical value. The minimum region is due to the fact that the mean free path of the electron is less for the thermal resistivity than for electrical resistivity. The Lorenz number for dysprosium as a function of temperature (Fig. 3) has some unusual features. First, the temperature variation is not at all of the standard type. Second, the value of the quantity L, especially at low temperatures, is much higher than that expected for pure electronic thermal conduction. Thus, we are forced to conclude that at low temperatures we have some additional transport carriers beside the electrons. In principle, the lattice and the magnon conductivity could be very likely responsible for the large Lorenz number. A contribution from magnons to the total thermal conductivity is not unreasonable because at low temperatures the magnon specific heat is large in comparison with the lattice specific heat.[18] The abrupt change in the thermal conductivity at the ferromagnetic-antiferromagnetic transition is believed to be due to the abrupt appearance of the magnetic superlattice energy gaps. Since these energy gaps decrease continuously to zero as one approaches the antiferromagnetic-paramagnetic transformation,[10] there is no abrupt change in the thermal conductivity at this transition.

[13] S. Arajs and R. V. Colvin, J. Less-Common Metals 4, 572 (1962).
[14] R. J. Elliott, Phys. Rev. 94, 564 (1954).
[15] J. M. Ziman, *Electrons and Phonons* (Oxford University Press, London, 1960).
[16] R. W. Powell, R. P. Tye, and M. J. Woodman, J. Less-Common Metals 5, 49 (1963).
[17] G. K. White and R. J. Tainsh, Phys. Rev. **119**, 1869 (1960).
[18] O. V. Lounasmaa and R. A. Guenther, in *Rare Earth Research*, edited by J. F. Nachman and C. E. Lundin (Gordon and Breach Science Publishers, New York, 1962), p. 197; Phys. Rev. **126**, 1357 (1962).